Proceedings of the Institute of Acoustics

TRANSMISSION OF NOISE THROUGH RUBBER-METAL COMPOSITE SPRINGS

A.H. Muhr

Malaysian Rubber Producers' Research Association. Brickendonbury. Hertford.

INTRODUCTION

In many cases of noisy machinery, the noise is largely generated by vibrational excitation of structures to which the machine is attached rather than by direct airborne transmission. Thus proper mounting of the machine should generally be undertaken to reduce such excitations before considering measures such as sound insulating enclosures [1].

The design principles of mounts for isolating vibrations of moderate frequency are well known, and a great variety of such mounts are available. Each type of mount offers a particular combination of damping and force-deformation behaviour (in the various directions) which makes it appropriate for some vibration isolation requirement. However, the implication of such design details for the transmission of audio-frequencies is often less certain. Although the general principles of audio-frequency transmissibility are available [1,2,3] the current emphasis in reducing noise requires more care be taken about the design details.

This is particularly true for the automotive industry, since the trend towards lighter structures exacerbates the problem of noise. The acoustical and vibrational characteristics of modern cars thus call for very careful tuning, which can lead to conflicting targets. For engine mounts, damping is required to control the large amplitude vibrations around 5-10Hz while in the acoustic frequency range (30Hz to around 1000Hz, excitation amplitude decreasing rapidly as frequency rises) high damping is undesirable [4].

In the simple theory of vibration isolation, it is assumed that the vibrations are unidirectional and the isolating spring has negligible mass. The function of the spring (in addition to being able to bear the static load) is to provide a low stiffness at the frequency of interest, so that the vibrating body exerts only a small dynamic force on the isolated body. For higher frequencies, additional mechanisms may cause the transmissibility to be higher than expected from the simple theory. Firstly, the inertia of the spring may become significant, and this could lead to resonances (due to wave effects) within the spring and consequent peaks of high transmissibility in the frequency range of interest. Secondly, there may be a tendency for the high frequency vibrations to occur in directions other than the main compliance of the isolating spring. If the spring is effectively rigid in these directions then there will be no attenuation of the vibrations. Thirdly, at high frequencies it may no longer be admissible to assume that the springs are the only compliant elements of the system. This last effect will be peculiar to a particular system, and is beyond the scope of the present discussion.

As a rule of thumb, rubber elements in suspension systems are believed to reduce transmission of noise (in comparison to a system consisting entirely of metal components). From the above discussion, two main ideas can be put forward as to why rubber elements should have this effect:

(i) Standing wave resonances may be damped by the internal damping in the rubber, or alternatively the waves may be reflected by interfaces between unlike materials such as rubber and metal. It is necessary to invoke such mechanisms because, in the absence of wave effects, a rubber spring should have higher transmissibility than a metal spring of the same stiffness because of the higher damping of the rubber.

(ii) Rubber elements usually have significant compliance in all directions. This mechanism will apply not only to rubber mounts, but also to elements such as rubber bushes in the eyes of leafsprings which will provide some longitudinal compliance and hence reduce transmission of longitudinal excitations.

As a start to clarify the status of the first mechanism, some measurements have been made on the unidirectional transmissibility of representative springs, using frequencies where wave effects occur. Before reporting the results it may be helpful to review and develop the appropriate theory.

THEORY

For simplicity, attention will be restricted to vibrations which are sinusoidal, steady state and unidirectional.

1. Single spring

The transmissibility T of the system depicted in Figure 1 is defined to be

$$T = \frac{|F_{out}|}{|F_{in}|} \tag{1}$$

where F_{out} is the force exerted by the spring on the rigid base, F_{in} is the force driving the mass 2M (say at a displacement of $u=u_\ell e^{j\omega t}$, that is amplitude u_ℓ and angular frequency ω) and absolute values have been taken because F_{out} and F_{in} are complex numbers. Using Newtons' second law, equation (1) may be rewritten as

$$T = \frac{|F(x=0)|}{|F(x=\ell)-M\omega^2|} \tag{2}$$

where F(x) is the amplitude of the force exerted by the spring to the right of the plane at x on the spring to the left of the plane at x.

When the inertia of the spring is negligible, F is independent of x, and assuming the spring to be linear in its force-deformation behaviour

$$F(x=0) = F(x=\ell) = k^* u_\ell \tag{3}$$

where $k^* = k' + jk''$ is the complex stiffness of the spring (the asterisk is a reminder that k^* is a complex quantity). Insertion of equation (3) into (2) leads to

$$T = \sqrt{\frac{k'^2 + k''^2}{(k'-M\omega^2)^2 + k''^2}} \tag{4}$$

which is the usual result. It should be noted that in general k' and k'' are functions of ω. It is a simple matter, using equation (4), to calculate T from measurements of M and the complex stiffness k^*.

The "complex stiffness" of the spring becomes an ambiguous term when there is significant internal inertia, since it depends which end of the spring is chosen for the force measurement. Moreover, since the modulus $E'+jE''$ of a rubber is in general a function of ω (and hence also is $k'+jk''$ even in the absence of inertial effects), $F(x=\ell)$ cannot be deduced from measurements of $F(x=0)$ over a range of frequencies. However, the transmissibility could be calculated using equation (2) (if M is known) from measurements of both $F(x=0)$ and $F(x=\ell)$.

If the stiffness of the spring is uniformly distributed, equation (3) may be replaced by

$$F(x) = k^*_L \,(du/dx) \tag{5}$$

where k^*_L is the complex stiffness a unit length of the spring would have in the absence of inertial effects. If the mass of the spring is also uniformly distributed, with mass ρ_L for a unit length, then use of equation (5) with Newton's second law applied to an elemental section dx of the spring leads to

$$(k^*_L/\rho_L)\partial^2u/\partial x^2 + \omega^2u = 0 \tag{6}$$

Equation (6) is just the displacement part of the wave equation in a dissipative medium, the solution to the wave equation having been treated as having the separable form $u(x)e^{j\omega t}$, and the wave velocity c being given by

$$c^2 = k'_L/\rho_L \tag{7}$$

Looking for solutions of (6) of the form

$$u(x) = e^{jnx} \tag{8}$$

leads to the conclusion that if $k''_L \neq 0$ then n is complex so that without loss of generality

$$n = p + jq \tag{9}$$

with p real and positive and q real (p may be taken as positive because if e^{jnx} is a solution of (6) it immediately follows that so is e^{-jnx}). Inserting (8) and (9) into (6) and equating real and imaginary parts leads to

$$n = \frac{\omega}{dc\sqrt{2}}\{\sqrt{d+1} - j\sqrt{d-1}\} \tag{10a}$$

$$\text{where } d = \sqrt{1 + k''^2_L/k'^2_L} = \sqrt{1 + \tan^2\delta} = \sec\delta \tag{10b}$$

As pointed out by Kolsky [5], the signs of the real and imaginary parts of n correspond to the physics of wave propagation in a dissipative medium, since a wave travelling in the positive x direction (in mathematical form, $e^{j(\omega t-nx)}$) will diminish in amplitude as x increases. Similarly the wave travelling in the opposite direction ($e^{j(\omega t+nx)}$) will also diminish in amplitude in the direction in which it is travelling.

The general solution of the wave equation may be expressed as a sum of waves travelling in each direction, with amplitudes such that the boundary conditions at x=0 (u=0) and $x=\ell$ ($u=u_\ell$) are met. However, it is mathematically more convenient to take the independent solutions to be u(x)=sin(nx) and u(x)=cos(nx) instead, since it is then immediately apparent that the solution to equation (6) is

$$u(x) = \frac{u_\ell}{\sin(n\ell)} \cdot \sin(nx) \tag{11}$$

Inserting equation (11) into equation (5) gives

$$F(x) = \frac{u_\ell}{\sin(n\ell)} \, k^*_L \, n\cos(nx) \tag{12}$$

so that equation (2) becomes

$$T = \frac{| k^*_L n/\sin(n\ell) |}{| k^*_L n\cos(n\ell)/\sin(n\ell) - M\omega^2 |} \tag{13}$$

Equation (13) has been presented before in different forms [1,2,3]. To evaluate the equation it should be noted that:

$$\begin{aligned} \cos(n\ell) &= \cos(p+jq)\ell = \cos(p\ell)\cosh(q\ell)+j\sin(p\ell)\sinh(q\ell) \\ \sin(n\ell) &= \sin(p+jq)\ell = \sin(p\ell)\cosh(q\ell)-j\cos(p\ell)\sinh(q\ell) \end{aligned} \tag{14}$$

Snowdon refers to equation (13) as being the solution for longitudinal waves in a long solid rod. For that case we may identify

$$\begin{aligned} k^*_L &= E^*A \\ \rho_L &= \rho A \end{aligned} \qquad \text{solid homogeneous spring} \tag{15}$$

where E^* is the (complex) Young's modulus, A is the cross sectional area and ρ is the material density. However, the formula is equally well applicable to a rubber simple shear spring, where the shear modulus G^* of the rubber must be substituted for E^* in the above formula, or to waves in a generalized spring which need not be solid (for example longitudinal waves in a coil spring [6]):

$$\begin{aligned} k^*_L &= k^*\ell \\ \rho_L &= m/\ell \end{aligned} \qquad \text{general spring} \tag{16}$$

where k^* is the (complex) stiffness the spring would have in the absence of inertial effects, m is the mass of the active part of the spring and ℓ is the active length.

2. Two springs in series

Application of the method described above to the system depicted in Figure 2 along with the appropriate boundary conditions at x = h:

$$\begin{aligned} u_1 &= u_2 \\ -k_1(\partial u_1/\partial x)+k_2(\partial u_2/\partial x)^1 &= -m_1\omega^2 u \end{aligned} \tag{17}$$

yields

$$\begin{aligned} F(x=0) &= \frac{k_1 n_1(\sin(n_2 h)+R\cos(n_2 h))u_\ell}{\sin(n_1 h)(\sin(n_2\ell)+R\cos(n_2\ell))} \\ F(x=\ell) &= \frac{k_2 n_2(\cos(n_2\ell)-R\sin(n_2\ell))u_\ell}{\sin(n_2\ell)+R\cos(n_2\ell)} \end{aligned} \tag{18}$$

$$\text{where } R = \frac{\omega^2 m_1\sin(n_2h)\sin(n_1h)-k_1n_1\cos(n_1h)\sin(n_2h)+k_2n_2\cos(n_2h)\sin(n_1h)}{-\omega^2 m_1\cos(n_2h)\sin(n_1h)+k_1n_1\cos(n_1h)\cos(n_2h)+k_2n_2\sin(n_2h)\sin(n_1h)}$$

and the subscripts 1, 2 indicate properties of springs 1 and 2 respectively. These formulae, together with equation 10 and 14 and their analogues, can be used to calculate T (defined in equation 2). For clarity the asterisks have been omitted, but k, n and R are in general complex quantities.

EXPERIMENTAL

A servohydraulic machine (Schenck VH7) was used to apply sinusoidal excitations in the frequency range 1-1000Hz to the upper surface of the test spring. The lower surface of the spring system was mounted on a piezoelectric load cell (Kistler 9321 A) which has negligible compliance for the present purposes. The input force was measured using a piezoelectric force link (Kistler 9061) mounted on the actuator. A suitable attachment (with a significant mass) was used between the force link and the spring. The transmissibility was determined from the ratio of these forces (measured by means of Kistler 5008Y4 charge amplifiers and a Solartron 1250 frequency response analyser) according to equation 1.

Two arrangements were investigated. In the first, rubber-steel laminates were deformed in a 3-point bend (Figure 1). For sufficiently large values of the distance between the loading points, the metal does not contribute to the stiffness but merely constrains the deformation of the rubber to be in simple shear [7]. It should therefore be possible to analyse the results using equation (15) but replacing E by G. In these experiments ℓ = 131mm, the rubber was 44.5mm wide and 14mm thick while the steel was 0.25mm thick. Three types of rubber were used (all unfilled): Natural Rubber (NR), 25% epoxidized Natural Rubber (ENR-25) and 50% epoxidized Natural Rubber (ENR-50). A summary of the rubber properties is given in Table 1. A static downward deflection of 7.5mm was applied to the springs throughout the dynamic tests (the dynamic deflections were in the range 0.2 - 0.05mm). The experimental results are compared in Figure 3 to the predictions of equation (13) using the properties of the rubbers interpolated linearly from the 50Hz and 400Hz data.

In the second arrangement (Figure 2), a coil spring (a six-turn valve spring from a motor car engine) was arranged in series with a pad either of NR or of ENR-50. The pads were 8mm thick and 25mm in diameter and were bonded top and bottom to aluminium plates (1.2mm thick). In addition, the transmissibility of the coil spring was measured without either rubber pad. The experimental results are compared in Figure 4 to the predictions of equation (18) using the properties of the rubbers interpolated linearly from the 50Hz and 800Hz data. A value of $\tan\delta = 0.005$ was used for the coil spring (this was the only parameter used for 'fitting' in the Figures).

DISCUSSION & CONCLUSIONS

It is apparent from Figure 3 that the laminates are behaving in the general manner expected from the theory, which treats them as being rubber springs. Thus the lightly damped NR spring shows clear peaks corresponding to the spring resonances, while as the damping is increased (from NR to ENR-25 to ENR-50) the peaks are progressively suppressed. The large peak around 640Hz (and the progressive divergence of theory and experiment as it is approached) in all three plots arises not from the rubber spring but from a resonance of the jig. The jig, in effect, is a stiff metal spring in series with the rubber spring in a manner analogous to Figure 2. The large peak around 15Hz in all cases arises from the 'simple theory' resonance of the attachment (mass 2M = 939g) on the spring. The discrepancies between theory and experiment for the higher order resonances of the NR laminate may arise from the effects of the overhang (22mm) and the finite bending stiffness of the metal layers.

The discrepancies in the peak position in Figure 4 may arise from uncertainties in the active mass and length of the coil (about 20% of the coil mass is located in the inactive end turns). A more serious and puzzling discrepancy between theory and experiment is the greater damping effect of the rubber pads on the spring resonance peaks than predicted. Nevertheless, the effect is not so gross as to suggest that a large difference in "characteristic impedances" (ie. $\sqrt{\rho E}$) between materials in the composite system investigated here is in itself enough to reduce noise transmission, although such a mechanism has sometimes been put forward [3,8]. Instead, it appears from the results that both high compliance and high damping are the required properties of the rubber pad.

TRANSMISSION OF NOISE THROUGH RUBBER-METAL COMPOSITE SPRINGS

REFERENCES

1. MacDuff, J.N. and Curreri, J.R. "Vibration Control", 1958. McGraw.Hill, p.363
2. Snowdon, J.C., "Vibration and shock in damped mechanical systems" 1968, John Wiley & Sons Inc., pp21-77
3. Payne A.R., Rubber Chem. & Tech. 1964, 37, 1190-1244
4. Haertel, V., Proc. UNIDO Workshop on Industrial Composites based on Natural Rubber, Joharta 1986, publ. MRRDB 1987, pp114-126
5. Kolsky, H. "Stress waves in solids" 1953, OUP pp116-122
6. Johnson, B.L. and Stewart, E.E., Transactions of the ASME, Journal of Engineering for Industry, 1969, 1011-1016
7. Muhr, A.H. and Thomas, A.G., To be published in Rubber Chem. & Tech., 1989
8. Oyadiji S.O. and Tomlinson, G.R., Proc. Institute Acoustics, 1980 p67-70

TABLE 1 Vulcanizate properties (measured using hardness buttons*)

Polymer	Frequency	phase angle	stiffness N/mm	deduced Young's Modulus (MPa)
NR	50	4	224	1.6
	400	7	247	1.8
	800	10	233	1.7
ENR-25	50	8	320	2.3
	400	20	430	3.2
	800	27	484	3.6
ENR-50	50	24	457	3.4
	400	40	975	7.2
	800	45	1286	9.7

* 25mm diameter, 8mm thickness, disc. In these experiments it was bonded to aluminium endpieces and statically precompressed to 80N before carying out the dynamic tests in compression (amplitude about ± 0.1mm).

FIGURE 1 Arrangement to measure the transmissibility of rubber–steel laminates

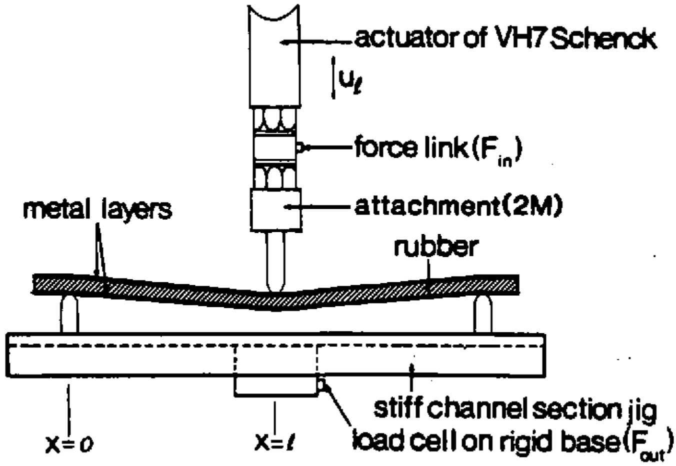

FIGURE 2 Arrangement to measure the transmissibility of two springs in series

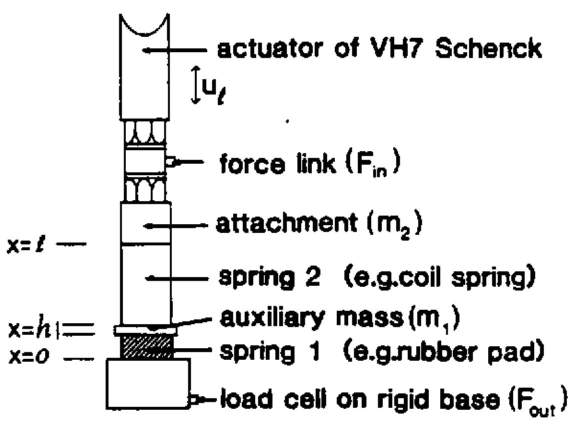

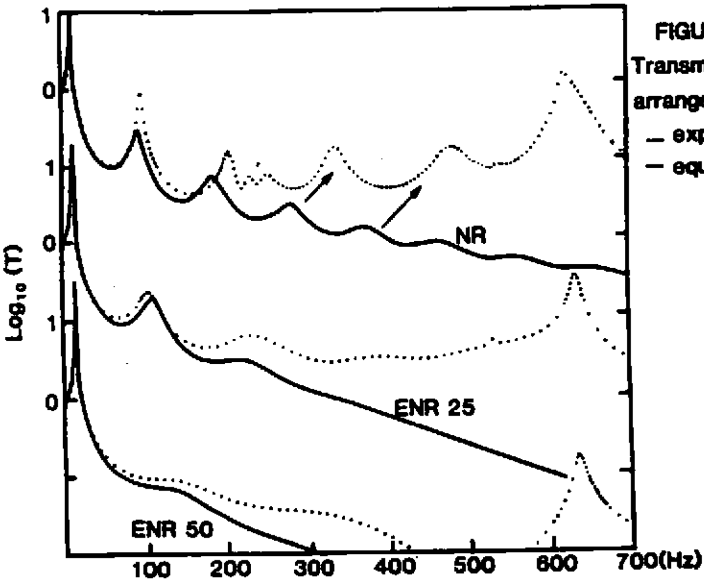

FIGURE 3
Transmissibility of the arrangement of Fig 1
_ experiment
— equation 16

FIGURE 4 Transmissibility of arrangement of Fig.2 _ experiment — equation 18

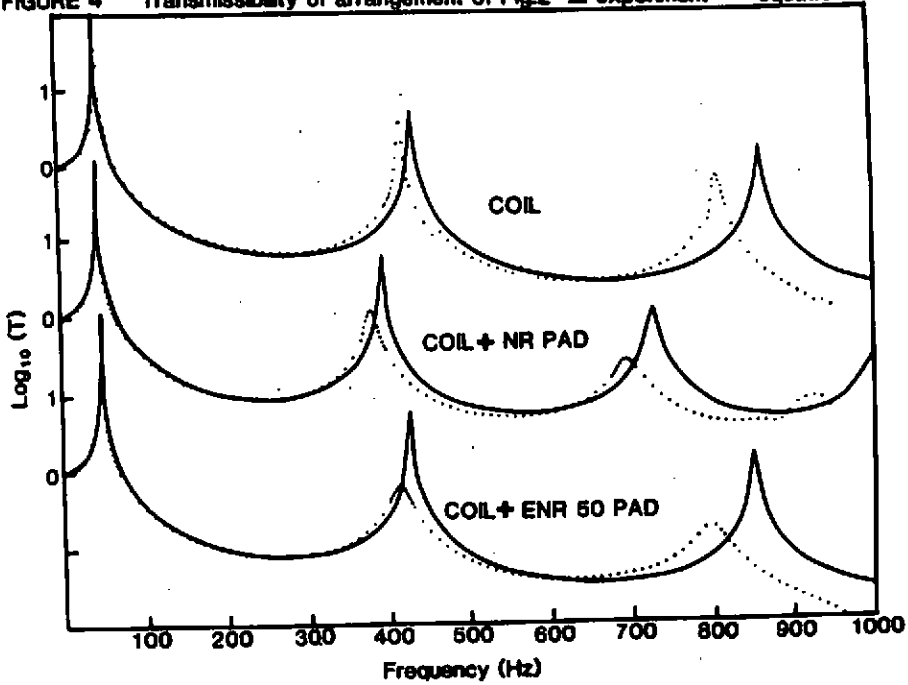

THE USE OF TIME REVERSED DECAY MEASUREMENTS IN SPEECH STUDIOS

Birgit Rasmussen[1] & Jens Holger Rindel[2]

1) Brüel & Kjær, DK-2850 Nærum, Denmark
2) The Acoustics Laboratory, Technical University of Denmark, DK-2800 Lyngby, Denmark

INTRODUCTION

In speech studios with reverberation times around 0,1 – 0,2 s it is not possible to use traditional measuring techniques because of the ringing of ¹/₃ octave filters. A new measuring technique, which is based on a time reversed analysis, has been used in three speech studios in the Danish Broadcasting House and the results have been compared with traditional methods. The interrupted noise method has been used, and the relation between limits for reliable results and the choice of measurement setup parameters has been closely regarded.

MEASUREMENT METHOD

A suitable and convenient measurement method is not found in any standard. The international standard ISO 3382 (1975) [1] describes field measurements of reverberation time, but guidelines for the measurement of short reverberation times are not included. Further, the standard is completely out-of-date, since the main contents is more than 15 years old, and the measurement technique has developed considerably during this period. Some useful hints are found in ISO 354 (1985) [2], but measurement of short reverberation times in studios is outside the field of application, and not possible using the method described. Consequently, the measurement procedure must be defined utilizing experience from other practical measurements and the new possibilities offered by modern instrumentation.

Interrupted noise excitation

In the traditional method a broadband noise source is used and after the source has been switched off the decay curve is recorded on a level recorder. However, this curve can have strong fluctuations due to the stochastic character of the excitation noise, and several decay curves should be evaluated in each position.

Using the measuring technique of today, the decay curve can be held in the memory of the instrument. This has made it possible to average the decay curves from repeated excitations to an ensemble averaged decay curve with much reduced fluctuations. An example is illustrated in Fig. 1.

Evaluation of decay curves

For many years the most widely used evaluation range has been 30 dB, but within the last years there has been a tendency to prefer an evaluation range of only 20 dB. The last version of ISO 354 [2] has followed that tendency.

Traditionally, the first part of the decay curve (5 dB or so) should not be used for the evaluation. In connection with short reverberation times there is a very good reason to let the evaluation start when the decay curve has decreased by a few dB, instead of starting a very short time after the excitation signal has been stopped, as actually proposed in ISO 354 [2]. The reason is, that ¹/₃ octave filters, which are normally used for this type of measurements, will give the signal a certain time delay, and this is not negligible in connection with short reverberation times at low frequencies. For the ¹/₃ octave filters in the B & K 2133 analyzer which is used for the measurements in the studios an average delay has been found:

$$T_{delay} \approx 6/f \tag{1}$$

where f is the centre frequency of the ¹/₃ octave filter. As an example the time delay in the 125 Hz ¹/₃ octave band will be around 50 ms, which is quite a lot in connection with the measurements described in this paper. The delay is visible comparing the filtered decay curve in Fig. 2b with the unfiltered time signal in Fig. 2a.

Spatial averaging

Using traditional methods, spatial averaging is performed by averaging the reverberation times from different source/microphone combinations. However, modern measuring techniques have made it possible to extend the ensemble averaging to include the spatial averaging, too. As demonstrated by [3] and [4], this method gives a rather smooth decay curve, which gives a precise description of the reverberation process in a particular room. Although these conclusions were related to long reverberation times in reverberation chambers, it seems reasonable to assume that the spatial ensemble averaged decay curve is a very good basis for the evaluation of reverberation time. An example is shown in Fig. 1c.

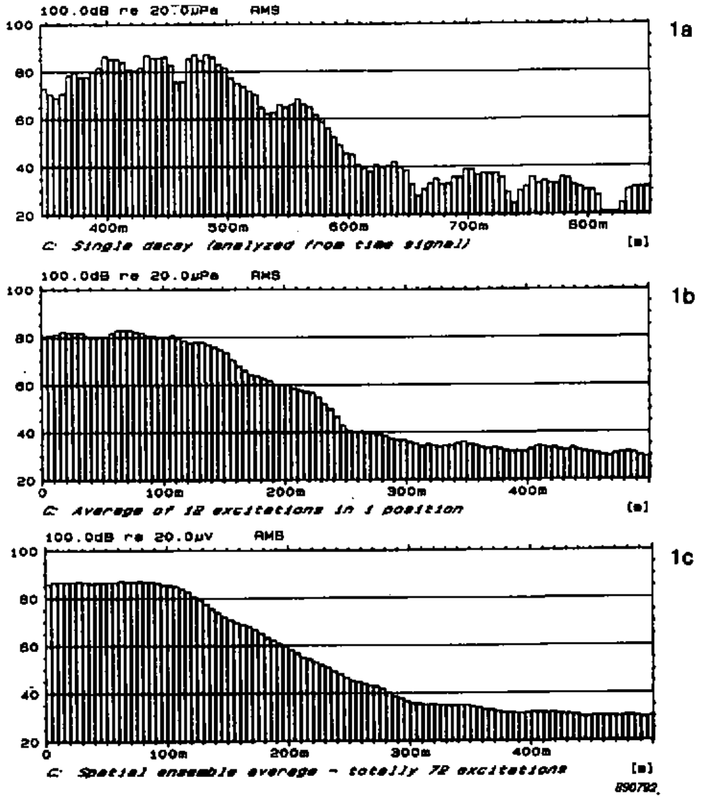

Fig. 1. Example of 1/3 octave decay measurements using noise excitation and ensemble averaging (49 m³ studio, 125 Hz)
a: Single excitation
b: Ensemble average of 12 excitations in 1 position
c: Spatial ensemble averaged decay curve using six source-microphone combinations, 72 excitations in total

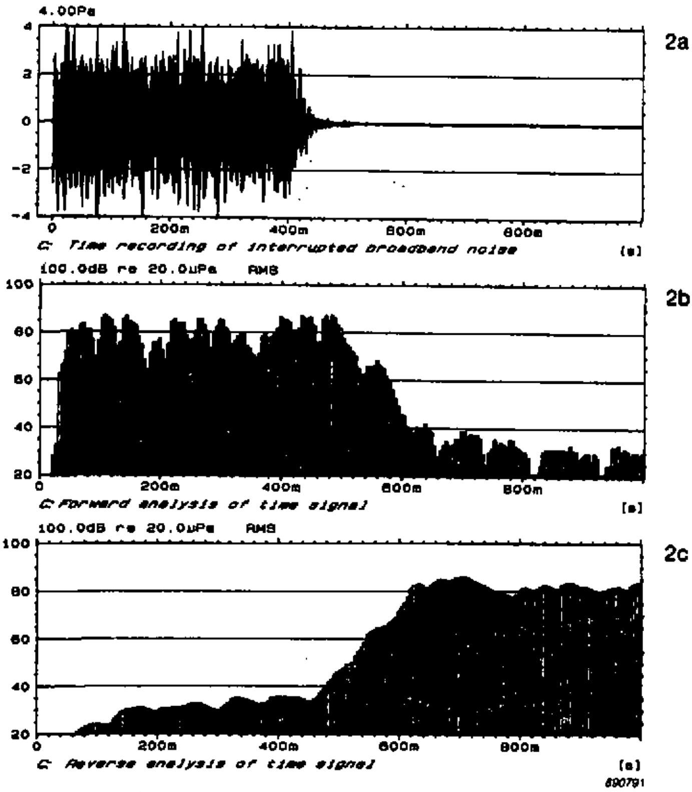

Fig. 2. Example of decay measurements using noise excitation
a: Time recording of interrupted broadband noise
b: Forward analysis of time recording, 1/3 octave, 125 Hz (T_{av} = 1/128 s)
c: Reverse analysis of time recording 1/3 octave, 125 Hz (T_{av} = 1/16 s)

PROBLEMS RELATED TO SHORT REVERBERATION TIMES

Using "classical" analysis technique, i.e. filtering in 1/3 or 1/1 octave bands, limitations exist due to "ringing" in bandpass filters and smoothing caused by the detector. The problems are further described below. The limitations caused by the filter occur when the absolute filter bandwidth is small, i.e. at low frequencies. The limit for the influence of the detector on the reverberation time is independent of frequency, but in practice most important at medium and high frequencies.

Limitations caused by bandpass filters

Reverberation time measurements are usually analyzed in 1/3 or 1/1 octave bands. However, such bandpass filters can influence the measurement due to filter ringing, which can give rise to characteristic waves in the decay, see Fig. 3. According to Ref. [5] reliable decay curves are obtained only if

$$B \cdot T_{60} > 16 \qquad (2)$$

where B is the bandwidth of the filter and T_{60} is the reverberation time to be measured. If requirement (2) is not met, the evaluated reverberation time depends very much on the evaluation range and can be too short or too long, i.e. the sign and size of the error is not predictable.

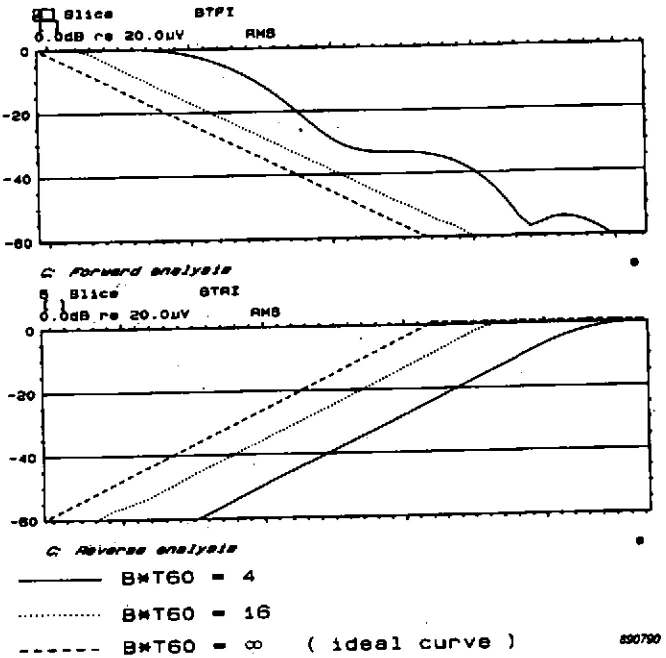

Fig. 3. Influence on decays of filter bandwidth.
Upper diagram: Forward analysis.
Lower diagram: Time-reversed analysis

However, in Ref. [6] it has been demonstrated that reversing the time signal to the filter leads to much less distortion of the decay curve. It has been found that if the upper 5 dB are excluded from the evaluation the requirement (2) can be replaced by

$$B \cdot T_{60} > 4 \qquad (3)$$

It should be noticed that there is no distinct limit between acceptable and unacceptable decay curves.

Limitations caused by detector
When measuring short reverberation times, it is important to choose the averaging time of the detector short enough to avoid influence on the decay curve. Using a device with exponential averaging (time constant τ_d) it has been shown in Ref. [5] that the averaging time should obey the requirement

$$T_{av} = 2\tau_d < T_{60}/14 \qquad (4)$$

Here again T_{60} is the reverberation time to be measured. If the requirement (4) is not met the evaluated reverberation time will be too long.

TIME REVERSED DECAY MEASUREMENTS

However, since the response of the detector is much faster when the signal increases instead of decreasing, it will be of great advantage to use time reversed analysis. According to Ref. [6] requirement (4) can then be replaced by

$$T_{av} = 2\tau_d < 8 \cdot T_{60}/14 \tag{5}$$

The influence of the detector is illustrated in Fig. 4 for forward as well as time reversed analysis. It can be seen that only the upper part of the decay curve is influenced when time reversed analysis and long averaging times are used. Further investigations reported in Ref. [7] have indicated that the reverberation times deviate less than 1% from the correct values, if conditions (2) – (5) are fulfilled, and the evaluation range does not include the upper 5 dB of the decay.

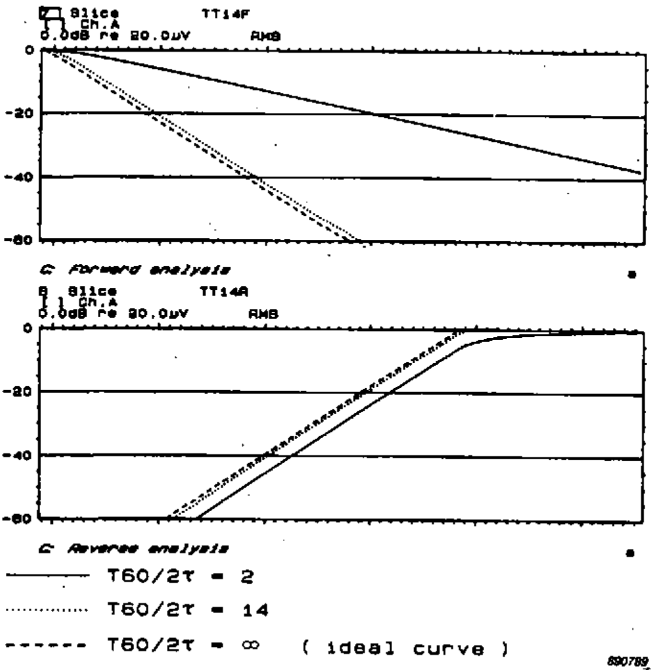

Fig. 4. Influence on decays of exp. averaging.
Upper diagram: Forward analysis.
Lower diagram: Time-reversed analysis

When a digital instrument is used, the choice of averaging time will also influence the lowest frequency band which can be used for measurements. In the B & K 2133 analyzer the sampling frequency is four times the centre frequency of the nearest octave band, f_{oct}, and the following requirement should be met

$$T_{av} \cdot f_{oct} \geq 1/4 \tag{6}$$

The averaging time is also connected to the frequency bands so that $B \cdot T_{av} \geq 1$ to obtain reliable results. This is a well known condition for the analysis of stationary signals, but at the first glance it could seem to be difficult to meet in decay measurements. However, ensemble averaging offers a solution to the problem: using this technique a requirement for the number of repeated and ensemble averaged excitations N_{exc} can be set up

$$N_{exc} \geq \frac{1}{B \cdot T_{av}} \tag{7}$$

To minimise the number of excitations, the averaging time should be as large as possible but still fulfill (4) or (5). Looking at these requirements, it is seen that a much larger averaging time is allowed for time reversed analysis than for forward analysis. Hence, fewer excitations are necessary, which is an additional feature of the time reversed analysis.

Limitations caused by sampling time interval

One of the advantages of exponential averaging is that it is possible to choose the time interval for sampling the decay curves, t_{samp}, independently from the averaging time. If at least n sample points are wanted for a regression line within the evaluation range D, the condition is

$$t_{samp} \leq T_{60} \cdot \frac{D}{n \cdot 60} \tag{8}$$

Typical values are $D = 20$ dB and $n = 3$ (2 being the absolute minimum for n).

DESCRIPTION OF THE STUDIOS

Three speech studios in the Danish Broadcasting House were selected as measuring objects because the reverberation times were expected to be very low. The volumes of the studios were 68 m^3, 49 m^3 and 36 m^3, respectively. The studios were furnished with a table and 4–6 chairs.

Two source positions were used, one of them close to a corner with the centre of the loudspeaker 0,4 m from each of the nearest surfaces. Three microphone positions were distributed in each room, 1,0 m, 1,2 m and 1,4 m above the floor. Each source position was used in combination with each microphone position, making a total of six combinations, which were used for spatial ensemble averaging.

INSTRUMENTATION AND MEASUREMENT SETUP

The measurements were carried out with the Brüel & Kjær Real Time Analyzer Type 2133. A more detailed description of the use of this instrument for measurement of short reverberation times is given in Ref. [7]. The important parameters which were chosen for the measurement setup are reported in Table 1. The averaging time of the detector has been chosen so, that the lower limit for accurate reverberation times is 0,11 s in all the measurements. In order to meet the requirement (7) at the lowest 1/3 octave band of interest, 50 Hz, a total of 12 excitations in each position were used for forward analysis. Only two excitations were required for reverse analysis, because a longer averaging time could be used.

Parameter	Eq.	Forward analysis	Reversed analysis
T_{av}		1/128 s	1/16 s
Min. T_{60}	(4), (5)	0,11 s	0,11 s
Lowest octave	(6)	31,5 Hz	4 Hz
Min. N_{exc} (50 Hz, 1/3 octave)	(7)	12	2
Max. t_{samp} (D = 10 dB, n = 3)	(8)	5 ms	5 ms

TB2102080

Table 1. Important parameters in the measurement setups for the three studios

MEASUREMENT RESULTS FROM THREE STUDIOS

The measured reverberation times in the three studios are shown in Fig. 5 The spatial ensemble averaged decay curves were evaluated over a range of 20 dB starting 5 dB below the steady state level. At very high and very low frequencies some of the results are missing because of insufficient signal-to-noise level. At most of these frequencies a value of the reverberation time could be found if the evaluation range was changed. The calculations of reverberation time are made utilizing a built-in function in the analyzer. Although individual evaluation ranges for each frequency can be specified in the analyzer, it was decided to use 20 dB evaluation range for all the results presented here.

Comparing the measured reverberation times with the limits imposed by the ringing of the 1/3 octave band filters (2) and (3), it is seen that only the values based on reversed analysis are reliable at the lower frequencies

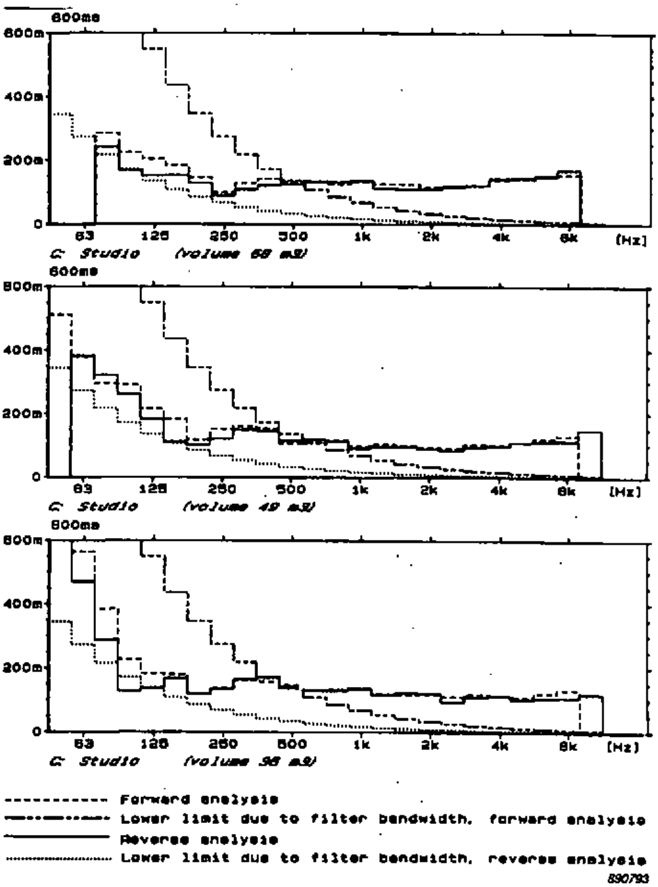

5a

5b

5c

Fig. 5. Measured reverberation times in three studios using forward and reverse analysis in 1/3 octave bands
a: 68 m³ studio
b: 49 m³ studio
c: 36 m³ studio

(below about 500 Hz). In all three studios there is a clear tendency that when the requirements for forward analysis are not met, the results are larger than those from reversed analysis. With a single exception the results from the reversed analysis are within all the requirements discussed above.

In addition to the measurements with interrupted noise a series of measurements was performed using impulse excitation and the technique of integrated impulse response. These results and a comparison of the measurement methods will be presented in another publication.

CONCLUSION

The measurement results from three speech studios have demonstrated that the ringing of 1/3 octave filters can introduce errors in the estimated reverberation times. These difficulties can be overcome when a time reversed analysis is used. In addition this method allows the number of excitations at each position to be reduced considerably.

REFERENCES

[1] ISO 3382 (1975). *"Acoustics – Measurements of reverberation time in auditoria"*

[2] ISO 354 (1985). *"Acoustics – Measurement of sound absorption in a reverberation room"*

[3] BODLUND, K. (1980). *"Monotonic curvature of low frequency decay records in reverberation chambers"*, J. Sound Vib. 73, pp.19–29

[4] BARTEL, T.W. & YANIV, S.L. (1982). *"Curvature of sound decays in partially reverberant rooms"*, J. Acoust. Soc. Am. 72, pp.1838–1844

[5] JACOBSEN, F. (1987). *"A note on acoustic decay measurements"*. J. Sound Vib. 115, pp. 163–170

[6] JACOBSEN, F. & RINDEL, J.H. (1987). *"Time reversed decay measurements"*, J. Sound Vib. 117, pp. 187–190

[7] RASMUSSEN, B. & PETERSEN, F. (1988). *"An automated instrumentation for measurements of very short reverberation times"*, WESTPAC III Conference, Shanghai, China, Proceedings pp. 929–932